Chiral Spin-Orbital Liquids with Nodal Lines

W. M. H. Natori,[1] E. C. Andrade,[1,2] E. Miranda,[3] and R. G. Pereira[1,4]
[1]*Instituto de Física de São Carlos, Universidade de São Paulo, C.P. 369, São Carlos, São Paulo 13560-970, Brazil*
[2]*Instituto de Física Teórica, Universidade Estadual Paulista, Rua Dr. Bento Teobaldo Ferraz, 271—Bloco II, 01140-070 São Paulo, São Paulo, Brazil*
[3]*Instituto de Física Gleb Wataghin, Unicamp, Rua Sérgio Buarque de Holanda, 777, CEP 13083-859 Campinas, São Paulo, Brazil*
[4]*International Institute of Physics, Universidade Federal do Rio Grande do Norte, 59078-970 Natal-RN, Brazil and Departamento de Física Teórica e Experimental Experimental, Universidade Federal do Rio Grande do Norte, 59072-970 Natal-RN, Brazil*
(Received 2 June 2015; revised manuscript received 13 February 2016; published 1 July 2016)

Strongly correlated materials with strong spin-orbit coupling hold promise for realizing topological phases with fractionalized excitations. Here, we propose a chiral spin-orbital liquid as a stable phase of a realistic model for heavy-element double perovskites. This spin liquid state has Majorana fermion excitations with a gapless spectrum characterized by nodal lines along the edges of the Brillouin zone. We show that the nodal lines are topological defects of a non-Abelian Berry connection and that the system exhibits dispersing surface states. We discuss some experimental signatures of this state and compare them with properties of the spin liquid candidate Ba_2YMoO_6.

DOI: 10.1103/PhysRevLett.117.017204

Quantum spin liquids (QSLs) are Mott insulators in which quantum fluctuations prevent long-range magnetic order down to zero temperature [1]. They have received both experimental and theoretical attention due to predictions of unusual phenomena such as spin-gapped phases with topological order or gapless phases without spontaneous breaking of continuous symmetries [2]. In recent years, the evidence for QSLs in nature has started to look more auspicious thanks to the discovery of new compounds that realize the Heisenberg model on frustrated lattices [3]. While frustration is a desirable ingredient, some seminal work by Kitaev [4] has demonstrated that bond-dependent exchange interactions may provide another route towards QSL ground states. The key idea is that a spin-1/2 model on the (bipartite) honeycomb lattice with judiciously chosen anisotropic interactions can be rewritten in terms of free Majorana fermions hopping in the background of a static Z_2 gauge field. The result is a QSL with exotic fractional excitations. The same idea has been applied to construct other exactly solvable models, including cases of higher spins [5–9].

From a broader perspective, Kitaev's model is an instance of a *quantum compass model* [10–12]. Although Kitaev-type exactly solvable models are artificial, the kind of anisotropic interactions they presuppose arises naturally in Mott insulators with orbital degeneracy and strong spin-orbit coupling [13,14]. There is recent evidence that bond-dependent interactions are dominant in Na_2IrO_3 [15]. While this compound is in a zigzag-ordered phase at low temperatures, the prospect of finding QSLs in compass models suggests inspecting other families of heavy-element transition metal oxides [16–18].

All of the conditions leading to quantum compass models can be found in Mott-insulating rock-salt-ordered double perovskites [19]. Given the chemical formula $A_2BB'O_6$, particularly interesting properties are found in compounds where the B' magnetic ions have a $4d^1$ or $5d^1$ configuration. These ions are arranged in a face-centered-cubic (fcc) lattice, which, unlike the honeycomb lattice, *is* geometrically frustrated. The magnetic properties within this family are diverse [20–23], but the material that stands out is Ba_2YMoO_6 [24–27]. Despite a Curie-Weiss temperature $\Theta_{cw} \approx -160$ K [24], several experiments point to the absence of long-range order down to $T \sim 2$ K. Moreover, there is no sign of structural transitions, implying that the lattice remains cubic at low temperatures. Thus, the degeneracy of the t_{2g} orbitals is only partially lifted by the spin-orbit coupling, leading to a low-lying $j = 3/2$ quadruplet [24]. The effective model contains bond-dependent interactions between nearest-neighbor $j = 3/2$ spins and is closely related to Γ-matrix generalizations of Kitaev's model [5,7]. Remarkably, the analysis in Ref. [19] revealed that, when the antiferromagnetic exchange is dominant, ordered phases become unstable against quantum fluctuations, making this an interesting place to look for QSLs.

In this Letter we investigate a QSL in a realistic model for double perovskites with strong spin-orbit coupling. Using a representation of $j = 3/2$ operators in terms of six Majorana fermions, we start by showing that a hidden SU(2) symmetry of the Hamiltonian becomes an explicit SO(3) symmetry for three of these fermions, whereas the other three exhibit a compass-model-type Z_3 symmetry. As the model is not exactly solvable, we proceed with a mean-field approach and propose a spin liquid ansatz that preserves the SO(3) and Z_3 symmetries. The ansatz breaks inversion and time reversal symmetry, thus describing a *chiral* spin liquid. Most interestingly, we find that the

excitation spectrum is gapless along *nodal lines*, which are vortices of a Berry connection in momentum space. This feature makes this chiral spin liquid a strongly correlated analogue of line-node semimetals and superconductors discussed in the context of topological phases of weakly interacting electrons [28–31] and photonic crystals [32]. Going beyond the mean-field level, we use variational Monte Carlo (VMC) techniques [33–35] to show that our spin liquid state yields a remarkably low energy and should be regarded as a competitive candidate for the ground state of the spin-orbital model. Finally, we argue that the vanishing density of states at low energies predicted by our theory can account for some unusual properties observed in Ba_2YMoO_6.

The spin-orbital model for cubic double perovskites with d^1 electronic configuration is given by [19]

$$H = J \sum_{\alpha,\langle ij\rangle\in\alpha} \left(\mathbf{S}_{i,\alpha}\cdot\mathbf{S}_{j,\alpha} - \frac{1}{4} n_{i,\alpha} n_{j,\alpha} \right) - \lambda \sum_i \mathbf{l}_i \cdot \mathbf{S}_i. \quad (1)$$

Here, $J > 0$ is the antiferromagnetic exchange between nearest-neighbor spins and $\lambda > 0$ is the atomic spin-orbit coupling. The index α labels both planes (XY, YZ, or XZ) and t_{2g} orbitals (d_{xy}, d_{yz}, or d_{xz}) [36]. The operators $n_{i,\alpha}$ and $\mathbf{S}_{i,\alpha}$ describe the number and the spin of electrons occupying the α orbital on site i, with the constraint $\sum_\alpha n_{i,\alpha} = 1$, and $\mathbf{l}_i$ is the effective $l = 1$ orbital angular momentum of the t_{2g} states [37]. The total spin on site i is $\mathbf{S}_i = \sum_\alpha \mathbf{S}_{i,\alpha}$.

In the regime $\lambda \gg J$, spin and orbital operators can be projected into the low-energy subspace of total angular momentum $j = 3/2$ [19]. The projected Hamiltonian $\tilde{H} = P_{3/2} H P_{3/2}$, where $P_{3/2}$ is the projector, contains multipolar interactions in terms of $\mathbf{J}_i = \mathbf{l}_i + \mathbf{S}_i$. Our first step is to introduce operators $\mathbf{s}$ and $\boldsymbol{\tau}$ at each site as

$$\mathbf{s} = \frac{1}{2}(-\Gamma^{23}, \Gamma^{13}, \Gamma^{12}), \quad \boldsymbol{\tau} = \frac{1}{2}(\Gamma^4, -\Gamma^{45}, \Gamma^5). \quad (2)$$

The notation refers to five Dirac Γ matrices given explicitly by

$$\Gamma^1 = \sigma^z \otimes \sigma^y, \quad \Gamma^2 = \sigma^z \otimes \sigma^x, \quad \Gamma^3 = \sigma^y \otimes \mathbb{1},$$
$$\Gamma^4 = \sigma^x \otimes \mathbb{1}, \quad \Gamma^5 = -\Gamma^1\Gamma^2\Gamma^3\Gamma^4, \quad (3)$$

where σ^a, $a \in \{x, y, z\}$ are Pauli matrices, and 10 matrices $\Gamma^{\mu\nu} \equiv [\Gamma^\mu, \Gamma^\nu]/(2i)$ [5,38]. The components of $\mathbf{s}$ and $\boldsymbol{\tau}$ satisfy the SU(2) algebra $[s^a, s^b] = i\epsilon^{abc} s^c$, $[\tau^a, \tau^b] = i\epsilon^{abc}\tau^c$, and $[s^a, \tau^b] = 0$. The relation between the basis of J^z and the basis $|s^z, \tau^z\rangle$, with $s^z, \tau^z \in \{+, -\}$, is $|J^z = \pm\frac{3}{2}\rangle = |\mp, +\rangle$, $|J^z = \pm\frac{1}{2}\rangle = |\pm, -\rangle$.

In the new representation, the projected Hamiltonian assumes a relatively simple form:

$$\tilde{H} = \frac{J}{9} \sum_{\langle i,j\rangle\in\alpha} \left(\mathbf{s}_i \cdot \mathbf{s}_j - \frac{1}{4} \right) (1 - 2\tau_i^\alpha)(1 - 2\tau_j^\alpha), \quad (4)$$

where τ^α's are given by $\tau^{xy} = \tau^z$, $\tau^{yz(xz)} = \frac{1}{2}(-\tau^z \pm \sqrt{3}\tau^x)$. A few comments are in order. First, Eq. (4) has the familiar form of a Kugel-Khomskii model [39,40]. However, here the Kugel-Khomskii coupling involves *pseudospins* $\mathbf{s}$ and *pseudo-orbitals* $\boldsymbol{\tau}$ defined in the $j = 3/2$ subspace, where the original spins and orbitals are highly entangled. Second, the Hamiltonian commutes with $\mathbf{s}_{\rm tot} = \sum_i \mathbf{s}_i$. This is a manifestation of the hidden global SU(2) symmetry discussed in Ref. [19]. This continuous symmetry is unexpected, given that spin-orbit coupling breaks the conservation of $\mathbf{J}_{\rm tot} = \sum_i \mathbf{J}_i$, but it appears in related models for t_{2g} orbitals [41] and at special points of the Kitaev-Heisenberg model [42]. Finally, the pseudo-orbital coupling has the form of a 120° compass model [12]. There is a Z_3 symmetry generated by $U_3 = e^{-i(2\pi/3)\tau^y_{\rm tot}}$, followed by a C_3 rotation of the α planes.

In analogy with the spin liquid in Kitaev's model [4], we now introduce a Majorana parton representation for the generators of SU(4) (i.e., the basis of $j = 3/2$ operators). We write $\mathbf{s}$ and $\boldsymbol{\tau}$ operators as [43–48]

$$s_j^a = -\frac{i}{4}\epsilon^{abc}\eta_j^b\eta_j^c, \qquad \tau_j^a = -\frac{i}{4}\epsilon^{abc}\theta_j^b\theta_j^c. \quad (5)$$

The components of $\boldsymbol{\eta}_j$ and $\boldsymbol{\theta}_j$ are Majorana fermions that obey $\{\gamma_j^a, \gamma_l^b\} = 2\delta_{jl}\delta^{ab}$, where $\gamma \in \{\eta, \theta\}$. As the signs of the fermions can be changed ($\boldsymbol{\eta} \to -\boldsymbol{\eta}$, $\boldsymbol{\theta} \to -\boldsymbol{\theta}$) without affecting the physical operators, this representation bears a Z_2 redundancy. To eliminate the extra states, one can impose the local constraint [45]

$$D_j \equiv i\eta_j^1\eta_j^2\eta_j^3\theta_j^1\theta_j^2\theta_j^3, \qquad D_j = 1 \quad \forall\ j. \quad (6)$$

With this constraint we have $s_j^a\tau_j^b = -\frac{i}{4}\eta_j^a\theta_j^b$, and Hamiltonian (4) becomes quartic in Majorana fermions:

$$\tilde{H} = -\frac{NJ}{6} + \frac{J}{36} \sum_{\langle i,j\rangle\in\alpha} \Bigg[\left(\sum_{a<b} \eta_i^a\eta_j^a\eta_i^b\eta_j^b \right) + (\eta_i^1\eta_i^2\eta_j^3 + \eta_i^2\eta_i^3\eta_j^1 + \eta_i^3\eta_i^1\eta_j^2)\bar{\theta}_j^\alpha + (i \leftrightarrow j) + \bar{\theta}_i^\alpha\bar{\theta}_j^\alpha\boldsymbol{\eta}_i\cdot\boldsymbol{\eta}_j - \theta_i^\alpha\theta_j^\alpha\theta_i^2\theta_j^2 \Bigg], \quad (7)$$

where N is the number of sites and θ^α and $\bar{\theta}^\alpha$ are defined by $\theta^{xy} = \theta^1$, $\theta^{yz(xz)} = \frac{1}{2}(-\theta^1 \mp \sqrt{3}\theta^3)$, and $\bar{\theta}^{xy} = \theta^3$, $\bar{\theta}^{yz(xz)} = \frac{1}{2}(-\theta^3 \pm \sqrt{3}\theta^1)$.

Hamiltonian (7) is invariant under global SO(3) rotations of the $\boldsymbol{\eta}$ vector. The couplings involving the components of $\boldsymbol{\theta}$ have only a discrete symmetry, namely, the octahedral point group symmetry O_h of the lattice. The latter contains the Z_3 that rotates θ^α and $\bar{\theta}^\alpha$ by 120° in the (θ^1, θ^3) plane. In

addition, $\tilde{H}$ is invariant under time reversal $T = Ke^{-i\pi J^y_{\rm tot}}$, where K denotes complex conjugation. In terms of Majorana fermions, $T = K\prod_j \theta^1_j \theta^3_j$.

Next, we perform a mean-field decoupling of Hamiltonian (7). This is equivalent to neglecting fluctuations of the Z_2 gauge field and yields qualitatively correct results as long as the system is in a QSL phase with deconfined Majorana fermions [43]. Our choice of mean-field ansatz is guided by the condition of preserving the SO(3) and Z_3 symmetries. This restricts the set of nonzero parameters $\langle \gamma^a_i \gamma^b_j \rangle$. We obtain

$$\begin{aligned}\tilde{H}_{\rm MF} = -\frac{NJ}{6} + \frac{J}{36}\sum_{\langle j,l\rangle\in\alpha} [i(2u_{jl} + \bar{w}^\alpha_{jl})\boldsymbol{\eta}_j \cdot \boldsymbol{\eta}_l \\ + 3iu_{jl}\bar{\theta}^\alpha_j \bar{\theta}^\alpha_l - iw^\alpha_{jl}\theta^2_j\theta^2_l - iv_{jl}\theta^\alpha_j\theta^\alpha_l \\ + 3u^2_{jl} + 3\bar{w}^\alpha_{jl}u_{jl} - w^\alpha_{jl}v_{jl}],\end{aligned} \tag{8}$$

where $iu_{jl} = \langle \eta^a_j \eta^a_l \rangle$, $iv_{jl} = \langle \theta^2_j \theta^2_l \rangle$, $iw^\alpha_{jl} = \langle \theta^\alpha_j \theta^\alpha_l \rangle$, and $i\bar{w}^\alpha_{jl} = \langle \bar{\theta}^\alpha_j \bar{\theta}^\alpha_l \rangle$ play the role of imaginary hopping amplitudes. Note that the symmetry implies a decoupling of η^a and θ^2 fermions at the level of bilinear terms; however, θ^1 and θ^3 remain coupled.

Seeking a translationally invariant ansatz, we set the order parameters to a uniform magnitude: $u_{ij} = u\sigma^u_{ij}$, $v_{ij} = v\sigma^v_{ij}$, $w^{xy}_{ij\in XY} = w\sigma^w_{ij}$, $\bar{w}^{xy}_{ij\in XY} = \bar{w}\sigma^{\bar{w}}_{ij}$, with u, v, w, $\bar{w}$ to be determined by self-consistent equations, whereas the σ's are chosen to be ± 1 on each bond. Since, e.g., $u_{ij} = -u_{ji}$, the choice of σ^u_{ij} is equivalent to a choice of bond orientation and determines the gauge-invariant flux through elementary plaquettes. Noticing that the fcc lattice can be viewed as a network of edge-sharing tetrahedra, we obtain a symmetric ansatz by requiring that the Z_2 fluxes, e.g., $\chi^u_{jkl} \equiv i\sigma^u_{jk}\sigma^u_{kl}\sigma^u_{lj}$, be the same on all faces of a given tetrahedron, with sites jkl on every triangle oriented counterclockwise with respect to an outward normal vector. This leads to the four-sublattice ansatz illustrated in Fig. 1.

Let us discuss the symmetry of our ansatz. First, we note that the Z_2 gauge flux through triangles is odd under time reversal and is related to the spin chirality order parameter [49,50]. The state also breaks inversion P; this can be seen from Fig. 1(b) since a mirror-plane reflection exchanges tetrahedra with opposite chiralities. Thus, our ansatz describes a chiral spin liquid with the spontaneous breaking of P and T. However, PT is still a symmetry. Similarly, a projective symmetry group analysis [2] shows that broken rotational symmetries can be combined with the broken time reversal to restore an O_h point group symmetry, ensuring the orbital degeneracy assumed at the outset (see the Supplemental Material [51]).

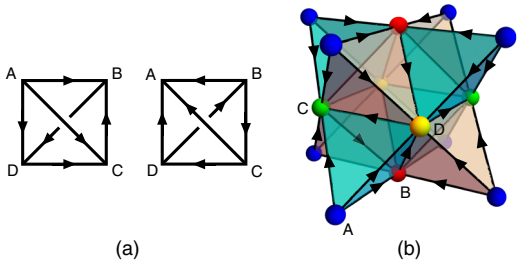

FIG. 1. (a) Two gauge-inequivalent hopping configurations with the same flux of the Z_2 gauge field on all faces of a tetrahedron. (b) Four-sublattice ansatz on the fcc lattice. The sign of the outward flux alternates between edge-sharing tetrahedra (represented by different color fillings).

Having fixed the ansatz, we can calculate the resulting spectrum of the Majorana fermions. For simplicity, first we focus on the mean-field Hamiltonian for $\gamma \in \{\eta^a, \theta^2\}$, i.e., the flavors which are decoupled in Eq. (8). In this case the Hamiltonian can be written in the form

$$\tilde{H}_{\rm MF} = \sum_{\mathbf{k}\in\frac{1}{2}\rm BZ} \gamma^\dagger_{\mathbf{k}} H(\mathbf{k}) \gamma_{\mathbf{k}} = |t| \sum_{\mathbf{k}\in\frac{1}{2}\rm BZ} \gamma^\dagger_{\mathbf{k}} (\mathbf{h}_{\mathbf{k}} \cdot \Sigma)\gamma_{\mathbf{k}}, \tag{9}$$

where $t = t(u, v, w, \bar{w})$ is the corresponding hopping amplitude in Eq. (8), $\gamma^\dagger_{\mathbf{k}} = (\gamma^\dagger_{\mathbf{k}A}, \gamma^\dagger_{\mathbf{k}B}, \gamma^\dagger_{\mathbf{k}C}, \gamma^\dagger_{\mathbf{k}D})$ is a spinor with components labeled by a sublattice index, $\mathbf{h}_{\mathbf{k}} = 4[\cos(k_x/2)\cos(k_y/2), \cos(k_y/2)\cos(k_z/2), \cos(k_z/2)\cos(k_x/2)]$, $\Sigma = (-\Gamma^1, -\Gamma^3, \Gamma^{13})$, and the sum is restricted to a half Brillouin zone since $\gamma_{-\mathbf{k}} = \gamma^\dagger_{\mathbf{k}}$ [44]. As the components of Σ obey $[\Sigma^a, \Sigma^b] = i\epsilon^{abc}\Sigma^c$, the spectrum is given simply by

$$\varepsilon_\pm(\mathbf{k}) = \pm|t||\mathbf{h}_{\mathbf{k}}|. \tag{10}$$

The dispersion relation is illustrated in Fig. 2. There are two doubly degenerate bands [51]. Since $\{P, \tilde{H}_{\rm MF}\} = 0$, the Hamiltonian has a chiral symmetry [52,53] and the spectrum is symmetric between positive- and negative-energy states. The defining feature of the band structure is the band touching along the edges of the Brillouin zone. These are nodal lines parametrized, e.g., by $\mathbf{k} = (\pi, \pi, k_z)$. Expanding $\mathbf{k} = (\pi + p_x, \pi + p_y, k_z)$, with $p_x, p_y \ll 1$, we obtain the effective Hamiltonian on a plane perpendicular to a line node: $H(\mathbf{k}) \approx 2|t|\cos(k_z/2)(p_x\Sigma^y + p_y\Sigma^z)$.

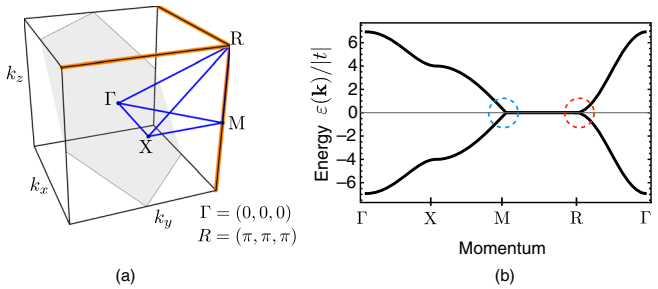

FIG. 2. (a) Brillouin zone of the cubic sublattice. (b) Bulk dispersion. The nodal lines along the MR directions cross at the quadratic band touching point R.

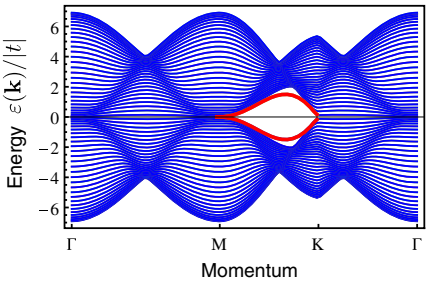

FIG. 3. Surface-state spectrum projected in the Brillouin zone of the triangular lattice for a (111) surface. The dispersion of the surface states corresponds to the thick red line between points M and K.

The latter is formally equivalent to the Hamiltonian for graphene and yields linear dispersion at low energies with k_z-dependent velocity $\varepsilon_{\pm}(\mathbf{k}) \approx \pm 2|t| \cos(k_z/2)\sqrt{p_x^2 + p_y^2}$. These nodal lines can be characterized as topological defects of an SU(2) Berry connection [54] in reciprocal space (see the Supplemental Material [51]). The three nodal lines related by C_3 symmetry cross at $R = (\pi, \pi, \pi)$. Expanding $\mathbf{k} = (\pi + p_x, \pi + p_y, \pi + p_z)$, we find that R is a quadratic band touching point [55,56] with anisotropic dispersion $\varepsilon_{\pm}(\mathbf{k}) \approx |t|\sqrt{p_x^2 p_y^2 + p_y^2 p_z^2 + p_x^2 p_z^2}$.

Another feature of topologically nontrivial states of matter is the presence of protected surface states. We identify the surface states by calculating the spectrum for $\tilde{H}_{\mathrm{MF}}$ in a slab geometry with open boundary conditions in the (111) direction (Fig. 3). There appear two pairs of doubly degenerate bands separated from the continuum, with dispersion terminating at the projections of the nodal lines. Remarkably, the positive-energy surface states are *spatially separated* from the negative-energy ones, as their wave functions are localized at opposite surfaces (the location of each state depends on the sign of the hopping parameter). This is a direct manifestation of the breaking of inversion symmetry.

We calculate the ground state energy E_{gs} at mean-field level by solving the self-consistent equations that determine the order parameters in Eq. (8). For this purpose, we had to diagonalize the Hamiltonian for coupled θ^1 and θ^3 fermions in Eq. (8) and found that the spectrum again displays nodal lines [51]. We obtain that $E_{\mathrm{gs}}^{\mathrm{MF}}/NJ \approx -0.248$. A better estimate of E_{gs} can be obtained by implementing a Gutzwiller projection according to Eq. (6) using VMC techniques [33,45]. Considering a restrictive form of the wave function which neglects variations in the population of the fermionic flavors (see the Supplemental Material [51]), we obtain that $E_{\mathrm{gs}}^{\mathrm{VMC}}/NJ = -0.40(1)$. This energy is already comparable to that of the best variational state identified in Ref. [19], namely, a valence bond solid with $E_{\mathrm{VBS}}/NJ \approx -0.417$. We expect the spin liquid to be stable since small fluctuations of the Z_2 gauge field only induce weak short-range interactions [2], which are irrelevant in the renormalization group sense for topological semimetals with point or line band touching in three dimensions [56].

The low-temperature thermodynamic properties are governed by the density of states $\rho(\varepsilon) \propto \sqrt{\varepsilon}$ of the Majorana fermions, which is due to the quadratic band touching point. It follows that the QSL has a heat capacity $C \propto T^{3/2}$, a magnetic susceptibility $\chi \propto T^{1/2}$, and a thermal conductivity $\kappa \propto T^{3/2}$ for $k_B T \ll J$. Another important property is the correlation function $G(\mathbf{r}) = \langle \mathbf{J}_j \cdot \mathbf{J}_{j+\mathbf{r}} \rangle$. We find that $G(\mathbf{r})$ vanishes when $\mathbf{r}$ connects sites on the same sublattice. For vectors connecting different sublattices along (100) directions in the form $\mathbf{r} = \boldsymbol{\delta} + r\hat{\mathbf{e}}$, where $\boldsymbol{\delta} \in \{(\frac{1}{2}, \frac{1}{2}, 0), (\frac{1}{2}, 0, \frac{1}{2}), (0, \frac{1}{2}, \frac{1}{2})\}$ and $\hat{\mathbf{e}} \in \{\hat{x}, \hat{y}, \hat{z}\}$, the correlation decays at large distances as $G(\mathbf{r}) \sim 1/r^4$. This power-law decay coincides with the result for a Dirac point in two dimensions [45].

Finally, we address the comparison with available experimental results for the spin liquid candidate Ba_2YMoO_6. Aharen *et al.* [25] observed that both the heat capacity and the magnetic susceptibility vanish at low temperatures, and they have attributed this behavior to a gapped collective spin singlet. de Vries *et al.* [24] proposed a picture of a valence bond glass but noted that the muon spin relaxation is comparable to that of QSLs [27]. Here, we propose that an alternative explanation for the vanishing heat capacity and susceptibility at low temperatures is the vanishing density of states of our *gapless* spin-orbital liquid with nodal lines. A comprehensive study of the properties of this QSL in comparison to experimental results will be presented elsewhere [57].

To summarize, we studied a realistic model for double perovskites in the regime of strong spin-orbit coupling. We proposed a new spin liquid ansatz that gives rise to nodal lines in the spectrum of Majorana fermions. We argued that some experimental results for Ba_2YMoO_6 can be interpreted in terms of the vanishing density of states predicted by our theory. We hope this work will stimulate the search for strongly correlated materials hosting fractional excitations with nontrivial momentum-space topology [48,58].

This work was supported by Brazilian agencies FAPESP (W. M. H. N., E. C. A.) and CNPq (E. M., R. G. P.).

[1] L. Balents, Nature (London) **464**, 199 (2010).
[2] X. Wen, *Quantum Field Theory of Many-Body Systems* (Oxford University Press, New York, 2004).
[3] T.-H. Han, J. S. Helton, S. Chu, D. G. Nocera, J. A. Rodriguez-Rivera, C. Broholm, and Y. S. Lee, Nature (London) **492**, 406 (2012).
[4] A. Kitaev, Ann. Phys. (Berlin) **321**, 2 (2006).
[5] H. Yao, S.-C. Zhang, and S. A. Kivelson, Phys. Rev. Lett. **102**, 217202 (2009).

[6] S. Mandal and N. Surendran, Phys. Rev. B **79**, 024426 (2009).
[7] C. Wu, D. Arovas, and H.-H. Hung, Phys. Rev. B **79**, 134427 (2009).
[8] M. Hermanns and S. Trebst, Phys. Rev. B **89**, 235102 (2014).
[9] K. O'Brien, M. Hermanns, and S. Trebst, Phys. Rev. B **93**, 085101 (2016).
[10] J. Dorier, F. Becca, and F. Mila, Phys. Rev. B **72**, 024448 (2005).
[11] C. Lacroix, P. Mendels, and F. Mila, *Introduction to Frustrated Magnetism: Materials, Experiments, Theory* (Springer, Berlin, 2011).
[12] Z. Nussinov and J. van den Brink, Rev. Mod. Phys. **87**, 1 (2015).
[13] G. Jackeli and G. Khaliullin, Phys. Rev. Lett. **102**, 017205 (2009).
[14] J. Chaloupka, G. Jackeli, and G. Khaliullin, Phys. Rev. Lett. **105**, 027204 (2010).
[15] S. Hwan Chun, J.-W. Kim, J. Kim, H. Zheng, C. C. Stoumpos, C. D. Malliakas, J. F. Mitchell, K. Mehlawat, Y. Singh, Y. Choi, T. Gog, A. Al-Zein, M. M. Sala, M. Krisch, J. Chaloupka, G. Jackeli, G. Khaliullin, and B. J. Kim, Nat. Phys. **11**, 462 (2015).
[16] D. Pesin and L. Balents, Nat. Phys. **6**, 376 (2010).
[17] X. Wan, A. M. Turner, A. Vishwanath, and S. Y. Savrasov, Phys. Rev. B **83**, 205101 (2011).
[18] W. Witczak-Krempa, G. Chen, Y. B. Kim, and L. Balents, Annu. Rev. Condens. Matter Phys. **5**, 57 (2014).
[19] G. Chen, R. Pereira, and L. Balents, Phys. Rev. B **82**, 174440 (2010).
[20] C. R. Wiebe, J. E. Greedan, G. M. Luke, and J. S. Gardner, Phys. Rev. B **65**, 144413 (2002).
[21] K. E. Stitzer, M. D. Smith, and H.-C. zur Loye, Solid State Sci. **4**, 311 (2002).
[22] K. Yamamura, M. Wakeshima, and Y. Hinatsu, J. Solid State Chem. **179**, 605 (2006).
[23] A. S. Erickson, S. Misra, G. J. Miller, R. R. Gupta, Z. Schlesinger, W. A. Harrison, J. M. Kim, and I. R. Fisher, Phys. Rev. Lett. **99**, 016404 (2007).
[24] M. A. de Vries, A. C. Mclaughlin, and J.-W. G. Bos, Phys. Rev. Lett. **104**, 177202 (2010).
[25] T. Aharen, J. E. Greedan, C. A. Bridges, A. A. Aczel, J. Rodriguez, G. MacDougall, G. M. Luke, T. Imai, V. K. Michaelis, S. Kroeker, H. Zhou, C. R. Wiebe, and L. M. D. Cranswick, Phys. Rev. B **81**, 224409 (2010).
[26] J. P. Carlo, J. P. Clancy, T. Aharen, Z. Yamani, J. P. C. Ruff, J. J. Wagman, G. J. Van Gastel, H. M. L. Noad, G. E. Granroth, J. E. Greedan, H. A. Dabkowska, and B. D. Gaulin, Phys. Rev. B **84**, 100404 (2011).
[27] M. A. de Vries, J. O. Piatek, M. Misek, J. S. Lord, H. M. Rønnow, and J.-W. G. Bos, New J. Phys. **15**, 043024 (2013).
[28] A. A. Burkov, M. D. Hook, and L. Balents, Phys. Rev. B **84**, 235126 (2011).
[29] C.-K. Chiu and A. P. Schnyder, Phys. Rev. B **90**, 205136 (2014).
[30] S. A. Yang, H. Pan, and F. Zhang, Phys. Rev. Lett. **113**, 046401 (2014).
[31] G. Bian *et al.*, Nat. Commun. **7**, 10556 (2016).
[32] L. Lu, L. Fu, J. D. Joannopoulos, and M. Soljacic, Nat. Photonics **7**, 294 (2013).
[33] C. Gros, Ann. Phys. (N.Y.) **189**, 53 (1989).
[34] D. Ceperley, G. V. Chester, and M. H. Kalos, Phys. Rev. B **16**, 3081 (1977).
[35] B. Edegger, N. Fukushima, C. Gros, and V. N. Muthukumar, Phys. Rev. B **72**, 134504 (2005).
[36] Y. Tokura and N. Nagaosa, Science **288**, 462 (2000).
[37] C. Ballhausen, *Introduction to Ligand Field Theory* (McGraw-Hill, New York, 1962).
[38] S. Murakami, N. Nagaosa, and S.-C. Zhang, Phys. Rev. B **69**, 235206 (2004).
[39] K. I. Kugel and D. I. Khomski, Sov. Phys. Usp. **25**, 231 (1982).
[40] L. F. Feiner, A. M. Oleś, and J. Zaanen, Phys. Rev. Lett. **78**, 2799 (1997).
[41] A. B. Harris, T. Yildirim, A. Aharony, O. Entin-Wohlman, and I. Y. Korenblit, Phys. Rev. Lett. **91**, 087206 (2003).
[42] J. Chaloupka and G. Khaliullin, Phys. Rev. B **92**, 024413 (2015).
[43] A. Tsvelik, *Quantum Field Theory in Condensed Matter Physics* (Cambridge University Press, Cambridge, England, 2007).
[44] P. Coleman, E. Miranda, and A. Tsvelik, Phys. Rev. B **49**, 8955 (1994).
[45] F. Wang and A. Vishwanath, Phys. Rev. B **80**, 064413 (2009).
[46] R. R. Biswas, L. Fu, C. R. Laumann, and S. Sachdev, Phys. Rev. B **83**, 245131 (2011).
[47] T. Herfurth, S. Streib, and P. Kopietz, Phys. Rev. B **88**, 174404 (2013).
[48] M. Hermanns, K. O'Brien, and S. Trebst, Phys. Rev. Lett. **114**, 157202 (2015).
[49] G. Baskaran, Phys. Rev. Lett. **63**, 2524 (1989).
[50] X. G. Wen, F. Wilczek, and A. Zee, Phys. Rev. B **39**, 11413 (1989).
[51] See Supplemental Material at http://link.aps.org/supplemental/10.1103/PhysRevLett.117.017204 for symmetry analysis, self-consistent equations for the mean-field ansatz, and variational Monte Carlo methods.
[52] X. Wen and A. Zee, Nucl. Phys. **B316**, 641 (1989).
[53] M. Koshino, T. Morimoto, and M. Sato, Phys. Rev. B **90**, 115207 (2014).
[54] F. Wilczek and A. Zee, Phys. Rev. Lett. **52**, 2111 (1984).
[55] K. Sun, H. Yao, E. Fradkin, and S. A. Kivelson, Phys. Rev. Lett. **103**, 046811 (2009).
[56] I. F. Herbut and L. Janssen, Phys. Rev. Lett. **113**, 106401 (2014).
[57] W. M. H. Natori *et al.* (to be published).
[58] J. Maciejko and G. A. Fiete, Nat. Phys. **11**, 385 (2015).